Proc. Natl. Acad. Sci. USA
Vol. 89, pp. 8671–8675, September 1992
Cell Biology

A membrane-based force generation mechanism in auditory sensory cells

FEDERICO KALINEC*, MATTHEW C. HOLLEY†, KUNI H. IWASA*, DAVID J. LIM*, AND BECHARA KACHAR*‡

*Laboratory of Cellular Biology, National Institute on Deafness and Other Communication Disorders, National Institutes of Health, Bethesda, MD 20892; and †Department of Physiology, The School of Medical Sciences, University Walk, Bristol, England BS8 1TD

Communicated by Thomas S. Reese, June 12, 1992

ABSTRACT **Auditory outer hair cells can elongate and shorten at acoustic frequencies in response to changes of plasma membrane potential. We show that this fast bidirectional contractile activity consists of an electromechanical transduction process that occurs at the lateral plasma membrane and can be activated and analyzed independently in small membrane patches inside a patch electrode. Bidirectional forces are generated by increases and decreases in membrane area in response to hyperpolarization and depolarization, respectively. We suggest that the force generation mechanism is driven by voltage-dependent conformational changes within a dense array of large transmembrane proteins associated with the site of electromechanical transduction.**

Mammalian outer hair cells (OHCs) generate high-frequency mechanical forces (1–4) that may refine the micromechanics of the basilar membrane (5–7). The mechanism of force generation is distributed along the lateral cell cortex (8), activated by changes of plasma membrane potential (4, 9, 10), and not directly dependent upon ATP (1).

Current models of force generation implicate all three of the main components of the lateral cortex, including the cortical cytoskeletal lattice (11, 12), the cortical endoplasmic reticulum, known as the lateral cisternae (3, 13), and the plasma membrane (14). The cortical lattice is a two-dimensional cytoskeleton that lies about 25 nm beneath the plasma membrane (11, 15–17). It is constructed from 5- to 7-nm circumferential filaments that are cross-linked at regular intervals by thinner filaments 60–80 nm long. The cross-links are aligned longitudinally with respect to the cell, and the possibility that they could generate charge-dependent length changes made them good candidates for the independent motor elements (11, 18). A quite different model is based upon the lateral cisternae, which lie immediately beneath the cortical lattice (19–21). In this model the cisternae form an essential component of a mechanism based upon electroosmosis (3, 13). Mechanisms proposed in association with the plasma membrane include changes of surface tension (8) and of surface charge (14). The plasma membrane almost certainly contains the voltage-sensitive part of the motor because the membrane potential field is practically limited to the lipid bilayer (22). Gating currents recorded from the membrane have a similar time course to length changes in isolated cells and may reflect electrical charge movements associated with voltage-sensitive membrane proteins (12, 22).

We now provide physiological evidence that the motor elements are located in the lateral plasma membrane and that they can be driven independently in isolated patches of plasma membrane observed inside the tip of a patch electrode. In conjunction with data from freeze-etching electron microscopy this evidence suggests that high-frequency forces are generated by conformational changes in a tightly packed array of voltage-sensitive, transmembrane proteins. Such a mechanism represents a form of membrane-based cell motility.

MATERIALS AND METHODS

Preparation of OHCs. Guinea pigs were decapitated following anesthesia with carbon dioxide. The bullae were removed and the cochlear spiral was dissected in Leibowitz L-15 cell culture medium. The organ of Corti was dissected from the cochlear spiral with a fine needle and dissociated mechanically by reflux through a pipette tip. The cells were allowed to settle in a 50-μl droplet of L-15 for 30 min on a clean glass coverslip.

Light Microscopy. An inverted Zeiss Axiomat microscope equipped with an internally corrected 100×, 1.3 numerical aperture (n.a.) planapochromatic objective was used in the differential interference contrast mode. The aperture of a 0.63 n.a. condenser was fully illuminated with a 100 W Hg lamp aligned for critical illumination (32). A video camera (DAGE-MTI, Michigan City, IN) and an optical memory disk recorder (Panasonic TQ-3031F) were used for contrast enhancement and recording. Displacement measurements were performed frame-by-frame from the recorded data using the image processing and analysis system IMAGE 1 (Universal Imaging, West Chester, PA).

Electron Microscopy. For freeze-fracture, organs of Corti were dissected from the cochlear spiral in L-15 and fixed by immersion in 2% glutaraldehyde in 0.1 M phosphate buffer, impregnated with 30% glycerol, frozen in liquid Freon 22, and freeze-fractured at −120°C in a Balzers 301 apparatus. For freeze-etching, organs of Corti were placed in low salt buffer (2.5 mM Na_2HPO_4/2.5 mM NaH_2PO_4/0.1 mM $MgCl_2$, pH 7.2) with 1% Triton X-100 and 33 nM rhodamine phalloidin (Molecular Probes) for 3 × 10 min. They were fixed in 2% glutaraldehyde in the low salt buffer, washed several times in distilled water, and rapidly frozen by contact with a liquid helium cooled copper block. Specimens were freeze-fractured at −150°C, allowed to etch for 10 min at −100°C, and rotary shadowed with platinum/carbon. Electron micrographs are shown in reverse contrast where platinum deposits appear white.

Electrophysiology. The whole cell variant of the patch-clamp technique was performed with an Axopatch-1D amplifier (Axon Instruments, Foster City, CA). Membrane potential was changed cyclically as a square waveform oscillating between +20 mV and −140 mV. Patch pipettes were pulled with a model P-87 Flaming-Brown puller (Sutter Instruments, Novato, CA) and positioned by an Eppendorf 5170 micromanipulator (Eppendorf). Pipettes were filled with intracellular solution containing 140 mM KCl, 2 mM $MgCl_2$, 0.28 mM $CaCl_2$, 0.5 mM EGTA, and 5 mM Hepes adjusted

The publication costs of this article were defrayed in part by page charge payment. This article must therefore be hereby marked "*advertisement*" in accordance with 18 U.S.C. §1734 solely to indicate this fact.

Abbreviation: OHC, outer hair cell.

‡To whom reprint requests should be addressed.

to pH 7.3 with KOH (8). Trypsin was purchased from Calbiochem.

RESULTS

OHCs isolated from the guinea pig cochlea are cylindrical with a uniform diameter of about 10 μm (Fig. 1*a*). Our experiments were conducted on cells isolated from the full length of the cochlea, with cell length ranging from 20 to 90 μm. Cell length changes (Fig. 1) were evoked by changing membrane potential via a patch electrode in the whole cell, voltage clamp mode applied to any point along the basolateral membrane (4, 8, 9).

To test the theory that forces are generated in the plasma membrane we disrupted the lateral cisternae and the cortical lattice in isolated OHCs by internally perfusing the cytoplasm with trypsin through a patch electrode. The sensitivity of the lattice to trypsin digestion was previously estimated from demembranated cells extracted with 2.5% Triton X-100 in low salt buffer (17). Unextracted cells were perfused with trypsin at 150 μg/ml for up to 40 min to maximize the probability of intracellular digestion. Formation and maintenance of the gigaohm seal condition throughout the length of these trypsin injection experiments were difficult. Perfusion of trypsin was assisted by applying cycles of positive and negative pressure to the fluid in the patch electrode. At each application of positive pressure the fluid volume injected into the cell was 5–10% of the total volume; thus the initial injection would have raised the intracellular trypsin concentration by up to 15 μg/ml. This exchange was repeated 5–10 times and intracellular digestion was followed for at least 40 min in 11 cells. The sequence of structural changes that characterize the intracellular disruption by the trypsin was distinctively apparent in the video images and was similar in all cells that were analyzed.

Before the intracellular trypsin digestion the cells were cylindrical, with the nucleus and other organelles in defined positions in the cytoplasm. The lateral wall complex consisting of the plasma membrane, the lateral cisternae, and the connecting cortical lattice (11–13, 16, 17) could be seen in the video images as a highly birefringent line. Often the lateral cisternae near the patch pipette detached and separated from the plasma membrane while the trypsin solution was being injected into the cell. During the first 10 min of a typical perfusion the cell progressively lost its shape (Fig. 2*a*) and many vesicular structures in Brownian motion appeared in the cytoplasm. The lateral cysternae disrupted into numerous

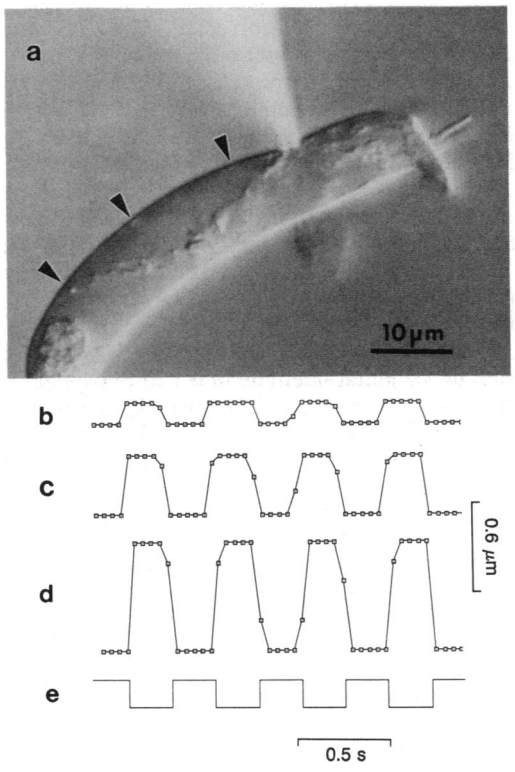

FIG. 1. An isolated OHC under whole cell voltage clamp. The shape changes of the cell were analyzed by tracing the position of organelles (arrowheads) located along the cell cortex in relation to the point at which the cell was held by the pipette. (*b–d*) Traces of organelle movements at progressive distances from the pipette. The amplitude of the movement is cumulative and increases proportionally to the distance to the point at which the cell is attached to the pipette. No relative displacements were detected at the basal (synaptic) region of the cell, which appears to move consistently as a unit. The cumulative nature of the response along the lateral wall and the absence of movement in the basal region of the OHC has been previously reported (8, 18).

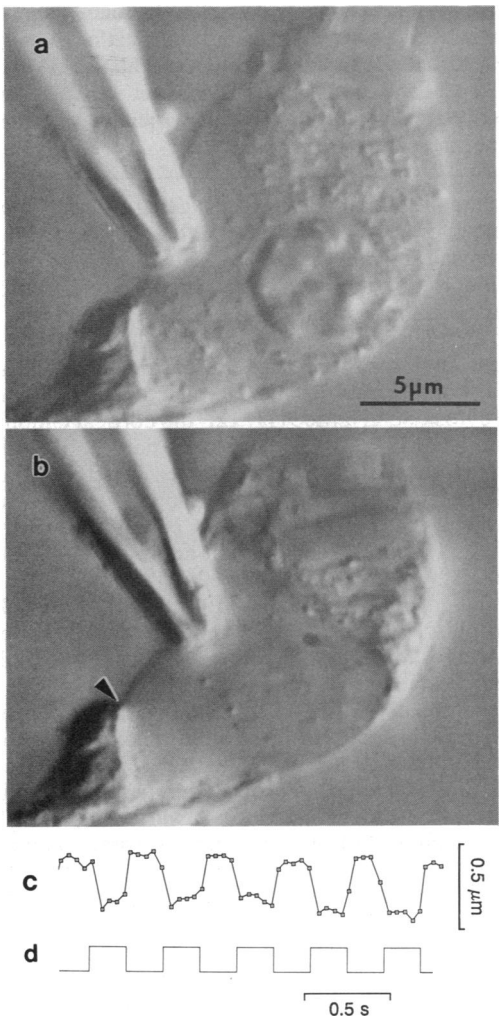

FIG. 2. An OHC, 40 μm long, perfused with trypsin at 150 μg/ml. The cuticular plate is to the top right of the image. (*a*) Five minutes after injection the cytoplasm structure was disrupted and the cell lost its regular cylindrical shape. (*b*) After 10 min the nucleus and most of the cytoplasm around the pipette were completely disrupted. Trypsin had no access to the efferent synaptic terminals in the lower left of the image and they remained unchanged. (*c*) Frame-by-frame analysis of the length changes of a clean profile of plasma membrane (from the pipette tip to the arrowhead, *b*) in response to a square wave stimulation (*d*). Similar results were obtained by perfusing trypsin into OHCs isolated from different turns of the cochlea.

small vesicles and the refractility of lateral wall decreased substantially. Within 10–30 min the nucleus completely disintegrated (Fig. 2*b*). Despite this progressive intracellular destruction voltage pulses continued to evoke pronounced changes of cell shape. Measurements of length changes in the membrane profile of the cell were done by tracing the position of debris of the synaptic terminals or of the Deiter cells still attached to the cell surface (Fig. 2*c*). Alternating membrane potential changes from +20 to −140 mV generated length changes of 5–6%, equivalent to those in normal cells (Fig. 2*c*). After 30–40 min these length changes were undiminished. Subsequent removal of the plasma membrane with 2.5% Triton X-100 showed no trace of the cortical lattice. If it had been present, it would have been conspicuous in images produced by video-enhanced microscopy (17). The dense actin networks in the stereocilia and cuticular plate did not show disaggregation within the 30–40 min of the experiment, probably reflecting limited diffusion rates in this part of the cell.

The behavior of membrane patches and the cellular distribution of the electromechanical transduction mechanism were studied by observing cell-attached patches with video-enhanced light microscopy. Patch electrodes with tip diameters of 1–2 μm and resistances of about 3–6 MΩ were attached to the cell membrane to form gigaohm seals (5–15 GΩ). These high-resistance seals remained constant throughout the experiment. Membrane potential was then alternated at 1–30 Hz as a square wave between a hyperpolarization and a depolarization of 80 mV from the holding potential (Fig. 3). The profiles of patches from any part of the lateral cell membrane were reversibly displaced inside the electrode in step with the command potential. Detailed analyses of video-recorded images showed that only 3 of 45 patches (one patch per cell) positioned along the lateral surface of the OHCs did not respond with measurable changes. The direction of the displacement depended upon the initial profile of the patch. If it was either concave or convex, then hyperpolarization accentuated the curvature, whereas depolarization reduced it. If the profile was initially flat, then following hyperpolarization it usually became concave or convex, but in some cases it buckled. During these observations the cell did not change shape. These results indicate that the electromechanical process that produces cell length changes can be activated locally along the lateral plasma membrane. The analyses of the dynamic video images provide convincing evidence that the membrane patches increase and decrease in surface area during hyperpolarization and depolarization, respectively (Fig. 3).

Patches derived from the basal, synaptic end of the OHC did not respond to changes of membrane potential. Only 2 of

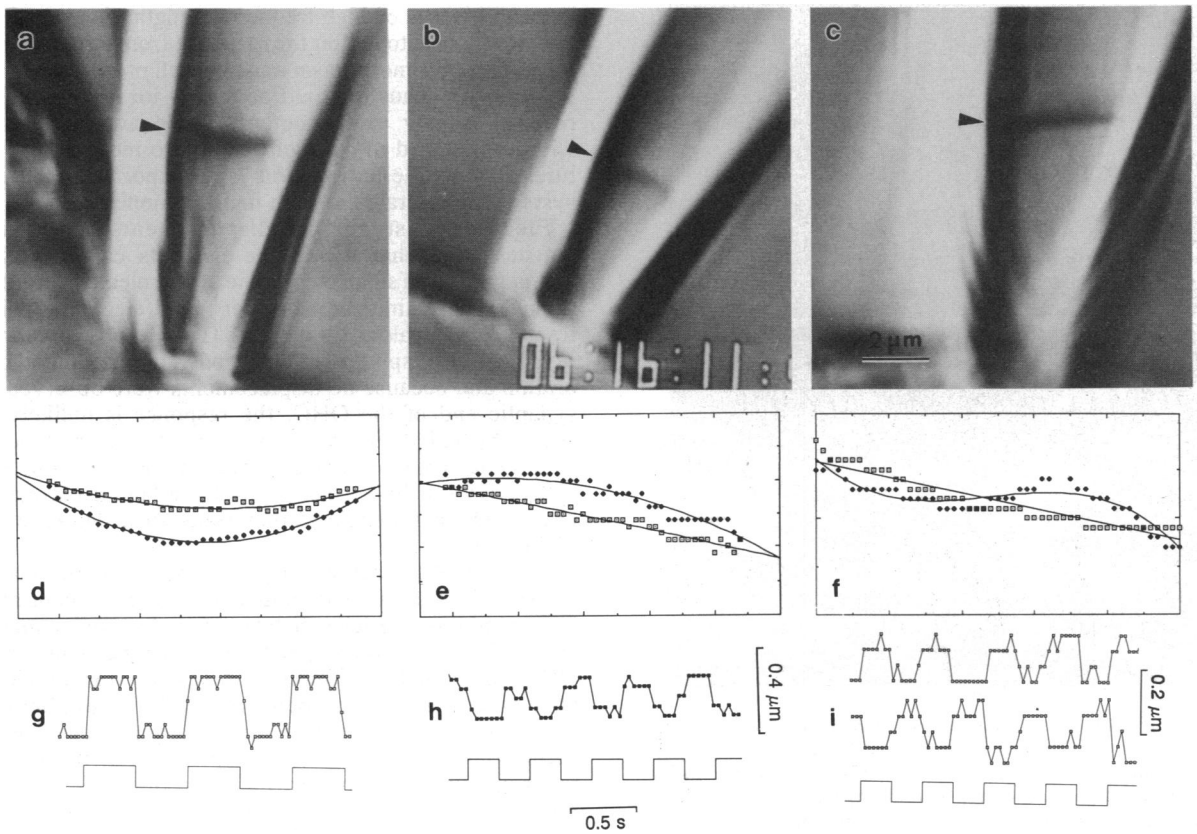

FIG. 3. Video images of the tight-sealed on-cell membrane patches showing three modes of the voltage-dependent membrane movement. (*a–c*) Images representing different membrane patches at 80 mV depolarization. To measure the changes in membrane area of the patch we determined the profile of the membrane patch as pixels with the local minima (of the pixel values) by scanning across the digitized images of the membrane. To illustrate the voltage-dependent movements of the membrane, the pixel tracing of the patches (*a–c*) at two membrane potentials (80 mV depolarization and 80 mV hyperpolarization) were superimposed in (*d–f*). On hyperpolarization (filled squares) the membrane patches moved downward (*d*), upward (*e*), or buckled (*f*), increasing their curvatures and membrane areas. These profiles were in most cases approximately arcs (*d* and *e*). The location where the sealed patch meets the inner surface of the pipette was, however, difficult to determine directly due to the 40° angle the pipette forms with the image plane and also due to the intense birefringence of the glass. We thus indirectly determined the border as crossing points of the arcs obtained by extrapolating the membrane profiles. From this analysis, the heights h, h', . . . of the arcs and the inner radius r of the pipette were obtained. The relative area change $\Delta S/S$ of the membrane patch can be determined from the generic formula $S = \pi(r^2 + h^2)$. The change in the membrane area was 6.3% for *d* and 3.3% for *e*. To show the response to voltage waveforms (bottom traces), the displacements of the center of the arc (patch *d* and *e*) in the pipette's axial direction was plotted (*g* and *h*, respectively). In the mode in which the center did not move (*f*), the movements of the two loops were plotted (*i*).

37 patches derived from positions basal to the nucleus showed the voltage-dependent displacements. No displacements were observed when the same patch conditions and electrical stimulation were applied to the lateral membrane of inner hair cells, Hensen cells, Deiter cells, or erythrocytes.

Images of the freeze-fractured protoplasmic face of the lateral plasma membrane between the apical tight junction belt and the level of the nucleus revealed a very high density of intramembrane particles (Fig. 4*a*). This area corresponded to the region of electromechanical transduction. Low-angle rotary shadowing of the true outer surface of the membrane emphasized a regular array of large, closely packed particles. This array resisted partial extraction of the membrane lipid with Triton X-100, a treatment that displayed individual particles more distinctly above the cortical cytoskeletal lattice (Fig. 4*b*). The array of particles was relatively regular; however the shape of each particle was difficult to determine in the replicas. The bulk portion of the particles had a diameter that ranged from 11 to 15 nm; however, platinum grains covering individual particles in the replica produced an irregular apparent diameter of up to 20 nm. The measured center to center distance between the particles in the array

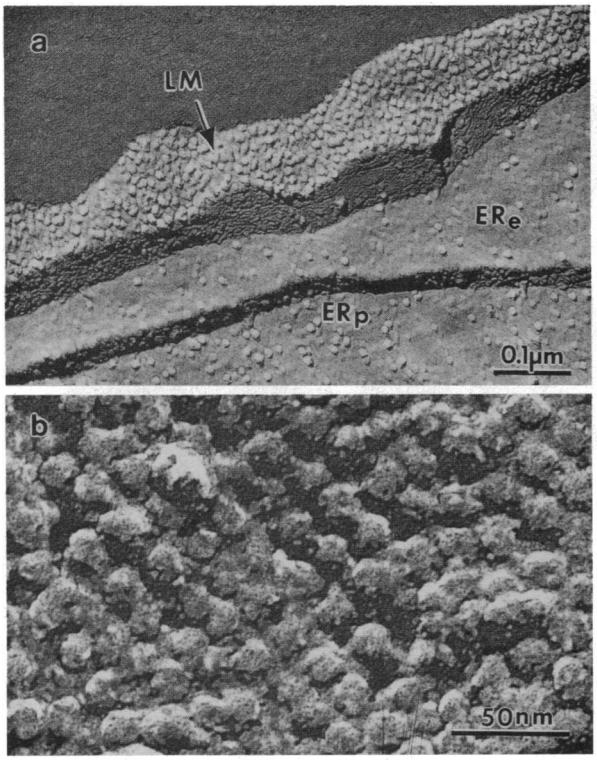

FIG. 4. Electron micrographs of replicas of the lateral plasma membrane of an OHC. (*a*) A conventional freeze-fracture replica showing the high density of integral membrane proteins in the protoplasmic fracture face of the lateral plasma membrane (LM) compared to the protoplasmic (ERp) and exoplasmic (ERe) fracture faces of the cisternal membranes. (*b*) Freeze-etched replicas of the lateral plasma membrane of an OHC partially extracted with Triton X-100 in low salt buffer. The rotary shadowed replicas of the true outer surface of the lateral plasma membrane showed large particles forming a regular array. Particle density was about 2500 per μm^2. The regular packing of these integral membrane proteins was not apparent in the freeze-fracture faces due to the plastic deformation during the fracture-replication procedure and to the presence of a large number of intercalated smaller intramembrane particles. The apparent larger size of the particles seen in the freeze-etching replica (*b*) in relation to the view in the freeze-fracture replicas (*a*) may reflect decoration of the particles with the detergent molecules. On the other hand, these complementary views may be genuinely revealing intramembrane and surface domains of the same molecules.

was 20.0 ± 0.2 nm (n = 50), which gives a spatial density of about 2500 per μm^2.

DISCUSSION

Previous experimental evidence has shown that the mechanism of force generation in OHCs lies along the lateral cortex (8, 18). Our experiments with trypsin suggest that it is specifically located in the lateral plasma membrane. Intracellular perfusion with trypsin extensively disrupted the lateral cisternae and the cortical lattice without inhibiting electromechanical transduction. The lateral cisternae are, therefore, unlikely to form an essential part of the mechanism. Furthermore, they are not electrically coupled to the plasma membrane (4), and their structural sensitivity (20) and variability (23) are inconsistent with the very robust nature of the motor (8).

The cortical lattice is also unlikely to act as a force generator. The intracellular concentration of trypsin was around 1000 times that required to digest the isolated lattice (17), and extraction of perfused cells with detergent provided direct evidence for intracellular digestion of the lattice. The lattice may be composed of the protein spectrin (11), which is particularly sensitive to trypsin digestion (24). Trypsin has often been applied extracellularly at concentrations of about 1 mg/ml to help dissociate hair cells from the organ of Corti prior to studies of high-frequency length changes. Since it apparently fails to inhibit the response from either side of the membrane, the mechanism must be well protected within the lipid bilayer. Thus it would be ideally located to sense and respond rapidly to the potential field across the bilayer without the need to pass information to more distant structures such as the lattice. This is an important feature for a system that operates at such high frequencies.

Electrically stimulated displacements of membrane patches show that the motor elements can be activated independently in small membrane areas selected at random in the plane of the membrane rather than "elementary circumferential rings" along the cell axis (18). Because the direction of membrane displacements depended on their initial configuration and because no displacements were observed at the synaptic end of the OHC, the response is unlikely to be caused by bulk fluid flow generated by the electric field inside the pipette. Thus we conclude that hyperpolarization leads to an increase in the surface area of the lateral plasma membrane, whereas depolarization leads to a decrease in the surface area.

Earlier freeze-fracture images of the lateral plasma membrane of OHCs revealed an unusually high concentration of intramembrane particles that were not observed in inner hair cells (25). The authors speculated that inner hair cells and OHCs may function differently in sensory transduction, but at that time the motile properties of OHCs were unknown and the membrane was presumed to have some specialized ionic permeability. We have extended this work by freeze-etching the membranes following partial extraction in detergent. The regular array of large intramembrane particles thus exposed could form the basis of a force-generating mechanism.

Each large membrane particle may possess a voltage sensor that can detect changes of membrane potential and lead either to conformational changes within the protein or to changes in protein packing within the array. It is clear from the behavior of voltage-gated ion channels (26, 27) and gap junctions (28, 29) that these are realistic mechanisms. Conformational changes of voltage-gated ion channels are associated with gating currents, which reflect the displacement of fixed charges across the membrane (26). In OHCs a similar movement of charges is associated with the changes of cell length (12, 22). The estimated maximum number of elementary charge movements varies from about 1000 per μm^2 (12)

to about 4000 per μm^2 (22). Assuming the density of voltage-sensitive particles in the array to be 2500 per μm^2 the estimated number of charges moved per particle would be 0.4–1.6, a range similar to that in voltage-gated ion channels (30, 31).

Membrane area changes and force generation may result from the cumulative (in series) action of the large number of elementary, independently activated, voltage-sensitive motors along the lateral plasma membrane. There is no evidence for specific interactions (33) between the large intramembrane particles, but the fact that their regular packing can resist Triton extraction suggests that they may be structurally linked. Furthermore, the array of membrane particles was not readily detached from the cortical cytoskeletal lattice by the Triton treatment (Fig. 4). The lateral plasma membrane is visibly connected to the cortical lattice by periodic protein pillars about 25 nm long (19). These pillars are attached only to the thicker, circumferentially oriented filaments of the lattice and not to the thinner, more elastic cross-links (11). Consequently, forces generated in the membrane should be constrained by a functionally anisotropic sheet whose stiffness is greater circumferentially than it is longitudinally (Fig. 5). Thus the intact cell is predisposed to change length rather than diameter. The magnitude of the change of surface area of patched membranes was calculated to be maximally 6–8%, which can account for the area change required to change cell length by 5%. The present study does not establish whether the membrane area changes are isotropic or anisotropic. The fact that the cell continues to change length after the trypsin digestion of the cortical lattice suggests that the membrane changes are anisotropic.

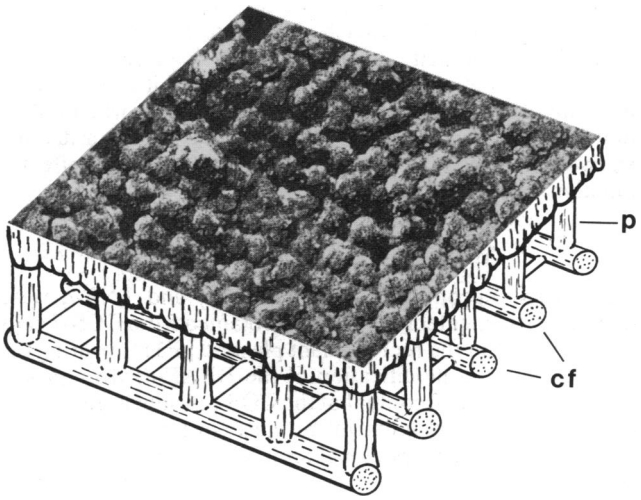

FIG. 5. Diagram in which an image of the etched particles from the plasma membrane is superimposed upon a diagram (11, 15, 16) of the cortical cytoskeletal lattice. Pillars (p) link the particles to the circumferential filaments (cf). Circumferential filaments are cross-linked by thinner, more elastic filaments up to 80 nm long, which are aligned with the longitudinal axis of the cell. Forces produced in the plane of the plasma membrane are thus directed along the axis of the cell to generate length changes.

In conclusion, the model we propose for the high-frequency mechanism of OHC motility involves a voltage-sensitive force generator that lies in the lateral plasma membrane. The specialized cortical cytoskeleton that lies beneath it is adapted to maintain the cylindrical shape of the cell and may ensure that forces produced in the membrane lead to changes of cell length.

We thank Dr. Jorgen Fex for critically reading this manuscript.

1. Kachar, B., Brownell, W. E., Altschuler, R. & Fex, J. (1986) *Nature (London)* **322,** 365–368.
2. Brownell, W. E., Bader, C. R., Bertrand, D. & de Ribaupierre, Y. (1984) *Science* **227,** 194–196.
3. Brownell, W. E. & Kachar, B. (1986) in *Peripheral Auditory Mechanisms*, eds. Allen, J. B., Hall, J. L., Hubbard, A., Neely, S. T. & Tubis, A. (Springer, Berlin), Vol. 64, pp. 369–376.
4. Ashmore, J. F. (1987) *J. Physiol. (London)* **388,** 323–347.
5. Corwin, J. T. & Warchol, M. E. (1991) *Annu. Rev. Neurosci.* **14,** 301–333.
6. Hudspeth, A. J. (1989) *Nature (London)* **341,** 397–404.
7. Ruggero, M. A. & Rich, N. C. (1991) *J. Neurosci.* **11,** 1057–1067.
8. Holley, M. C. & Ashmore, J. F. (1988) *Proc. R. Soc. London Ser. B* **232,** 413–429.
9. Santos-Sacchi, J. & Dilger, J. P. (1988) *Hear. Res.* **35,** 143–150.
10. Iwasa, K. & Kachar, B. (1989) *Hear. Res.* **40,** 247–254.
11. Holley, M. C. & Ashmore, J. F. (1990) *J. Cell Sci.* **96,** 283–291.
12. Ashmore, J. F. (1989) in *Cochlear Mechanisms: Structure, Function and Models*, eds. Wilson, J. P. & Kemp, D. T. (Plenum, London), pp. 107–114.
13. Dieler, R., Shehata-Dieler, W. E. & Brownell, W. E. (1991) *J. Neurocytol.* **20,** 637–653.
14. Jen, D. H. & Steele, C. R. (1987) *J. Acoust. Soc. Am.* **82,** 1667–1678.
15. Bannister, L. H., Dodson, H. C., Astbury, A. F. & Douek, E. E. (1988) *Prog. Brain Res.* **74,** 213–219.
16. Arima, T., Kuraoka, A., Toriya, R., Shibata, Y. & Uemura, T. (1991) *Cell Tissue Res.* **263,** 91–97.
17. Holley, M. C., Kalinec, F. & Kachar, B. (1992) *J. Cell Sci.* **102,** 569–580.
18. Dallos, P., Evans, B. N. & Hallworth, R. (1991) *Nature (London)* **350,** 155–157.
19. Flock, A., Flock, B. & Ulfendahl, M. (1986) *Arch. Otorhinolaryngol.* **243,** 83–90.
20. Evans, B. N. (1990) *Hear. Res.* **45,** 265–282.
21. Saito, K. (1983) *Cell Tissue Res.* **229,** 467–481.
22. Santos-Sacchi, J. (1991) *J. Neurosci.* **11,** 3096–3110.
23. Furness, D. N. & Hackney, C. M. (1990) *Eur. Arch. Otorhinolaryngol.* **247,** 12–15.
24. Speicher, D. W., Morrow, J. S., Knowles, W. J. & Marchesi, V. T. (1980) *Proc. Natl. Acad. Sci. USA* **77,** 5673–5677.
25. Gulley, R. L. & Reese, T. S. (1977) *Anat. Rec.* **189,** 109–124.
26. Liman, E. R., Hess, P., Weaver, F. & Koren, G. (1991) *Nature (London)* **353,** 752–756.
27. Armstrong, C. M. (1981) *Physiol. Rev.* **61,** 644–683.
28. Hanna, R. B., Ornberg, R. & Reese, T. S. (1985) in *Gap Junctions*, eds. Bennett, M. V. L. & Spray, D. C. (Cold Spring Harbor Lab., Cold Spring Harbor, NY), Vol. 20, pp. 23–32.
29. Deleze, J. (1987) *Experientia* **43,** 1068–1075.
30. Conti, F. & Stuhmer, W. (1989) *Eur. Biophys. J.* **17,** 53–59.
31. Zagotta, W. N. & Aldrich, R. J. (1990) *J. Gen. Physiol.* **95,** 29–60.
32. Kachar, B., Bridgman, P. C. & Reese, T. S. (1987) *J. Cell Biol.* **105,** 1267–1271.
33. Changeux, J.-P., Thiéry, J., Tung, Y. & Kittel, C. (1967) *Proc. Natl. Acad. Sci. USA* **57,** 335–341.